

GROUND-BASED RADIOMETRIC OBSERVATIONS OF EMISSION AND  
ATTENUATION AT 20.6, 31.65, AND 90.0 GHz

Ed R. Westwater, Jack B. Snider, and Michael J. Falls

NOAA/ERL/Wave Propagation Laboratory  
Boulder, Colorado 80303

Abstract--During 1987, ground-based zenith-viewing observations of atmospheric thermal emission were made at frequencies of 20.6, 31.65, and 90.0 GHz. At the locations of the experiments, San Nicolas Island, California, and Denver, Colorado, radiosonde observations of temperature and humidity were also available. The data, after conversion to attenuation using the mean radiating temperature approximation, are processed to derive attenuation statistics. In addition, both clear and cloudy attenuation characteristics are examined and compared with the most recent theories. Finally, the predictability and interdependence of the three separate channels are examined.

## 1. Introduction

Over the past decade, the Wave Propagation Laboratory (WPL) has designed, constructed, and field-tested several ground-based microwave radiometers to observe the atmosphere (Hogg et al., 1983; Westwater and Snider, 1987). In particular, extensive experience has been gained by using both zenith-viewing and steerable dual-frequency instruments operating at 20.6 and 31.65 GHz. These instruments continue to provide unique and meteorologically useful observations of precipitable water vapor (PWV) and integrated cloud liquid. Perhaps equally as useful, but certainly not as well studied, are the microwave attenuation characteristics that these devices can easily provide. Within the last year, WPL extended its radiometric capabilities by adding a channel at 90.0 GHz to the steerable and transportable radiometer. All three channels have equal beamwidths of 2.5 degrees, point in the same direction from the same location, and hence, are capable of simultaneously measuring emission and attenuation from the same volume of air. We present here examples of some of the data taken with the new system; from these data, several statistical and physical quantities, relevant to radio propagation studies, are derived and compared with theory.

## 2. Description of Experiments

## 2.1 San Nicolas Island, California, July 1987 (SNI)

In July 1987, WPL participated in an investigation of the characteristics of marine stratocumulus clouds at San Nicolas Island (SNI), located approximately 50 nautical miles west of Los Angeles. Observations of zenith brightness temperatures were made continuously by the WPL mobile, microwave radiometer operating at 20.6, 31.65 and 90.0 GHz. Although the primary purpose of the SNI observations was to study cloud properties, a secondary goal was the acquisition of statistics on attenuation by cloud liquid water, especially at 90.0 GHz. Supporting data for the attenuation measurements at SNI consisted of radiosondes launched up to several times daily and standard surface meteorological observations.

Clouds were persistent during the three week measurement period, being present for 76 percent of the time. Precipitable water vapor (PWV) was variable ranging from about 0.9 to 3.1 cm with a mean value of 1.9 cm.

## 2.2 Denver, Colorado, December 1987 (DEN)

The mobile three-channel radiometer was installed at the Denver (DEN) National Weather Service Forecasting Office (NWSFO) in December 1987, where it operated alongside the WPL six-channel radiometer (PROFILER) which measures PWV, cloud liquid, and temperature profiles. At Denver, supporting data were provided by the PROFILER, by the daily radiosondes released at standard times of 00 and 12 GMT, and by surface meteorological data. Denver weather in December is characterized by relative dry periods (PWV  $\leq$  0.5 cm) with occasional periods of snow. Clouds containing supercooled liquid water are common, especially prior to the onset of and during precipitation.

In contrast to SNI, clouds were present only 15 percent of the time. The PWV was low, ranging from 0.1 to 1.0 cm with a mean value of 0.5 cm.

## 2.3 General

Radiometers are calibrated using the "tipping curve" or elevation scan method in which absolute absorption at each operating frequency is calculated from the slope of the relative absorption versus relative path length (air mass) measured as the radiometer antenna is scanned in elevation (Hogg et al., 1983). Tipping curve calibrations are performed only during clear weather. The radiometer output at each operating frequency is related to the atmospheric brightness temperature calculated from the absolute absorption (in nepers) by

$$T_b = 2.75 e^{-\tau} + (1 - e^{-\tau})T_{mr} \quad (1)$$

where  $T_{mr}$  is a mean radiating temperature of the atmosphere and 2.75 is the cosmic background brightness (both in K).  $T_{mr}$  is normally calculated from climatological radiosonde data and was done so for DEN. For SNI, however,  $T_{mr}$  was computed from the 69 soundings recorded during July, 1987. The absorptions discussed in parts 4 to 6 are presented in dB which have been computed from the measured brightness temperatures by

$$\tau(\text{dB}) = 4.343 \ln \frac{T_{mr} - 2.75}{T_{mr} - T_b} \quad (2)$$

where the variables are defined in (1).

It should be noted that different humidity sensors were employed by the radiosondes at SNI and DEN. Soundings at SNI were made using Vaisala RS80 radiosondes with HUMICAP humidity sensors. At DEN standard VIZ radiosondes with "yellow element" humidity sensors were employed. Accuracies of 2 percent are claimed by both manufacturers. However, to the authors' knowledge, a rigorous intercomparison of the two units has not been made.

Representative brightness temperatures measured simultaneously at each operating frequency are shown in the time series of Fig. 1 for SNI and DEN. The maxima and higher scintillation rates are associated with liquid-bearing

clouds. Note the relative increase in 90 GHz brightness temperature as clouds pass through the radiometer antenna beam.

### 3. Attenuation Statistics

The time series of the data was edited in several ways before statistics were computed. First, 24-hr time series of all data were plotted and then visually inspected for the presence of outliers or questionable points. For Denver data, measurements at 20.6 and 31.65 GHz were also available from an adjacent radiometer; these also were used in visual editing. After the preliminary editing was completed, computer screening, based on approximately known physical relationships between the frequencies, was performed. This additional screening eliminated, for example, a segment of data in which snow on the antenna adversely affected the 90.0 GHz channel. After these stringent procedures were applied, there remained a total of 4805 5-min average data for SNI (about 400 hr) and 14181 2-min average data for DEN (about 473 hr). The cumulative probability distributions for the two data sets are shown in Figs. 2 and 3. At all frequencies, the mean attenuation at SNI is about a factor of 2 to 3 higher than at DEN. Several climatic factors are responsible for the differences between the two locations. First, the sea level altitude of SNI results in the dry attenuation always being greater than that at DEN. Second, the mean absolute humidity in SNI is a factor of three higher than at DEN, resulting in a much higher vapor absorption. Finally, the marine stratocumulus clouds of SNI contained measureable liquid 76 percent of the time and were only rarely present at temperatures below 0.0 degrees Celsius; the winter clouds at DEN contained measurable liquid about 15 percent of the time and were frequently supercooled. We are anticipating a completely different set of statistics when we operate at Denver during summer 1988.

### 4. Clear Air Absorption: Modeling Versus Experiment

The dominant microwave absorption from atmospheric gases in the troposphere arises from water vapor and oxygen, and the modeling of this absorption over the frequency range of 1 to 1000 GHz has been extensively studied by Liebe (1985). For water vapor, Liebe's model uses the known properties of all  $H_2O$  spectral lines below 1000 GHz and a Van Vleck-Weisskopf line shape to calculate the absorption. In addition, a "continuum" term, that accounts for contributions from lines above 1000 GHz, as well as from possible dimer contributions, is added to the line contribution. We used data from a recent publication of Liebe and Layton (1987) to model  $H_2O$  absorption, as a function of pressure, temperature, and water vapor pressure. Oxygen absorption was modeled using Liebe's formulas and computer software, but with an updated version of  $O_2$  interference coefficients given by Rosenkranz (1988). Our experience has been that the wing absorption at 20.6, 31.65, and 90.0 GHz is sensitive to the value of the  $O_2$  interference coefficients. For example, the constants given by Liebe and Layton gave rise to calculated brightness temperatures at 90.0 GHz that differed from our measurements (and from calculations based on Rosenkranz's values) by about 5 degrees. However, Liebe's and Layton's constants gave slightly better agreement at 20.6 and 31.65 GHz. Thus, for very precise calculations, such as are required in remote sensing, further study may be necessary.

We calculated brightness temperature from radiosonde soundings of temperature, pressure, and water vapor pressure as a function of height.

Since radiosondes do not measure cloud liquid, only data taken under clear conditions can be used for comparison. Tables 1 and 2 show mean and rms differences of measured and calculated brightness temperatures at SNI and DEN.

It is apparent from these tables that the agreement between theory and experiment in calculating clear air brightness temperatures is not completely satisfactory. Fairly substantial differences in the mean brightness temperature are present. However, the low standard deviations of the measurements suggest that the differences may be due to modeling the almost constant dry term. When comparing radiometer measurements with parameters derived from radiosondes, it should always be kept in mind that there are differences in the volumes of air sampled between the two instruments, and that the radiosonde itself is not a perfect instrument. Nevertheless, it seems that the mean differences between theory and experiment are significant, and that minor adjustments in parameters may be necessary.

## 5. Observations of Attenuation from Clouds

When attempting to verify calculations of microwave emission and attenuation from clouds, a limitation has been that conventional radiosondes do not measure cloud liquid. Even if they did, the highly variable temporal and spatial characteristics of clouds would make comparisons difficult. With our radiometer design of equal beamwidths at all three channels, emission from a common volume can be observed simultaneously. The problem then is to remove oxygen and water vapor emission when clouds are present, and then study the relative cloud effects between the three channels. The procedure that we use is straightforward and seemingly effective. We first establish a lower cloud liquid threshold  $L_t$  for the presence of clouds using the 20.6 and 31.65 GHz channels. In the past, this threshold has proven to be effective in separating clear and cloudy conditions. Next, we derive the precipitable water vapor  $V$  from the dual-channel measurements. This determination of  $V$  has been extensively verified by comparison with radiosondes, and, indeed, is of the same order of accuracy as the radiosonde. For data, whose inferred cloud liquid  $L$  is less than  $L_t$ , the "clear" set, we derive a regression relation between the measured absorption  $\tau_{clr}$  and  $V$ :

$$\tau_{clr} = A + BV. \quad (3)$$

The frequency dependent coefficients  $A$  and  $B$  in (3) have the physical significance of dry attenuation and mass absorption coefficient. Finally, for the data set whose inferred  $L$  is greater than  $L_t$ , the "cloudy" set, we determine the cloud attenuation  $\tau_{cld}$  by

$$\begin{aligned} \tau_{cld} &= \tau - \tau_{clr} \\ &= \tau - A - BV \\ &= C + DL. \end{aligned} \quad (4)$$

The coefficient  $D$  has the physical significance of the mass-absorption coefficient for cloud liquid, while if the procedure of subtracting clear from cloud attenuation were perfect,  $C$  would be zero. It should be understood that  $V$  in (3) has been derived from the measured 20.6 and 31.65 absorptions in cloudy conditions. We also derive  $L$ , but of course the accuracy of this determination has not been experimentally established, although theoretical estimates yield an accuracy of 0.0033 cm rms (Ciotti et al., 1987). Our

results on the relationships between attenuation at the various frequencies will be shown in Section 6; here, in Tables 3 and 4, we will present the results of our regression analyses to determine A, B, C, and D.

The calculations presented in these tables show that there is reasonable agreement between modeling and experiment, but also that, at Denver, in December, where the surface pressure is around 830 mb and the surface temperatures are frequently below zero, perhaps additional refinements are necessary. Since cloud liquid attenuation is sensitive to temperature, perhaps the disagreement between measurements and calculations at 90.0 GHz is significant. We intend to study this as more data become available.

## 6. Predictability of Attenuation Between Various Frequencies

There exists a fairly extensive amount of brightness temperature data at 20.6 and 31.65 GHz. Since data at 90.0 GHz are not plentiful, and certainly, simultaneous measurements at all three frequencies are scarce, it is of interest to examine their between-channel predictability. Such considerations are of importance when trying to estimate attenuation at various locations, but also for multi-frequency remote sensing, when the consideration of dependent channels is of utmost importance. We determined regression relations between the various channels for clear, cloudy, and all conditions. The form of the linear regression is

$$\tau \text{ (dependent)} = c_0 + c_1 \tau_1 \text{ (independent)} + c_2 \tau_2 \text{ (independent)}.$$

The results of the regression analyses are shown in Tables 5 and 6.

It is clear from Tables 5 and 6 that there is a high degree of predictability between the channels, and that if care is taken to distinguish between clear and cloudy conditions, the correlation coefficients are greater than about 0.90 for the linear regression equations.

## 7. Conclusions

Atmospheric attenuation at 20.6, 31.65, and 90.0 GHz has been derived from ground-based zenith-viewing microwave radiometers. These radiometers have equal beamwidths at all frequencies and simultaneously view the same common volume of atmospheric emitters. Calibration procedures for these radiometers utilize the "tipping-curve" method, and are independent for each channel. Measurements at two climatically different locations and months, San Nicolas Island, California, July 1987, and Denver, Colorado, December, 1987, have shown reasonable consistency between theory and experiment, both in clear air and during cloudy conditions. During clear conditions, comparisons between measured brightness temperatures and those calculated from on-site radiosondes, have average differences less than 2.9 K and standard deviations less than 1.2 K. The average differences may be due to uncertainties in calculating the wing contribution to absorption from the 60 GHz molecular band of oxygen. We used the most recent absorption models of Liebe and Layton (1987) and Rosenkranz (1988) when calculating absorption and emission from radiosondes. The ratios of cloudy attenuation values are reasonably consistent between the two locations. Probability distributions for attenuation were derived for the two climatologies, and as expected, San Nicolas Island had higher attenuation at all three frequencies than Denver.

Finally, we examined the inter-frequency predictability of the data and demonstrated that any two of the channels could significantly predict the remaining one (correlation coefficients greater than 0.90). This predictability was based on stratifying the data sets into clear and cloudy samples and then using linear regression analysis.

#### References

- Hogg, D.C., F.O. Guiraud, J.B. Snider, M.T. Decker and E.R. Westwater, "A Steerable Dual-Channel Microwave Radiometer for Measurement of Water Vapor and Liquid in the Troposphere," J. Appl. Meteor., vol. 22, pp. 789-806, May 1983.
- Liebe, H.J., "An Updated Model for Millimeter Wave Propagation in Moist Air," Radio Sci., vol. 20, pp. 1069-1089, Sept.-Oct. 1985.
- Liebe, H.J. and D. H. Layton, "Millimeter-Wave Properties of the Atmosphere: Laboratory Studies and Propagation Modeling," NTIA Report 87-24, pp. 1-80, October 1987.
- Rosenkranz, P.W., "Interference Coefficients for Overlapping Oxygen Lines in Air," J. Quant. Spectrosc. Radiat. Transfer, vol. 39, pp. 287-297, 1988.
- Westwater, E.R. and J.B. Snider, "Microwave Radiometer Facilities at the Wave Propagation Laboratory," Proceedings of NAPEX XI, JPL D-4647, pp. 24-27, Aug. 1987 (JPL internal document).

Table 1. Comparison between measurements and calculations of  
brightness temperature. San Nicolas Island, California,  
July 1987, Sample size = 14

	20.6 GHz	31.65 GHz	90.0 GHz
mean difference (K)	2.88	1.80	1.39
standard deviation (K)	0.65	0.32	1.16

Table 2. Comparison between measurements and calculations of  
brightness temperature. Denver, Colorado  
December 1987, Sample size = 22

	20.6 GHz	31.65 GHz	90.0 GHz
mean difference (K)	1.68	1.08	0.46
standard deviation (K)	0.72	0.33	0.97

Table 3. Regression relationships between zenith absorption (dB),  
precipitable water vapor V (cm), and integrated cloud liquid  
L (cm). San Nicolas Island, California, July 1987

clear conditions  
( $L < 0.0033$  cm)  
(N = 3417)

	20.6 GHz	31.65 GHz	90.0 GHz
A (dB)	0.0494	0.1281	0.2392
B (dB/cm)	0.1974	0.0787	0.3328
corr. coef.	0.9995	0.9811	0.9705

clear conditions  
(calculated from 14 radiosondes)

A (dB)	0.0812	0.1333	0.2387
B (dB)	0.1759	0.0782	0.3488
corr. coef.	0.9797	0.9595	0.9518

cloudy conditions  
( $L > 0.0033$  cm)  
(N = 14168)

C (dB)	0.0055	0.0073	0.0183
D (dB/cm)	3.5582	8.1057	45.2292
corr. coef.	0.9338	0.9662	0.9926

Table 4. Regression relationships between zenith absorption (dB), precipitable water vapor V (cm), and integrated cloud liquid L (cm). Denver, Colorado, December, 1987

---

clear conditions				
(L < 0.0033 cm)				
(N = 12015)				
	20.6 GHz	31.65 GHz	90.0 GHz	
A (dB)	0.0499	0.1073	0.1881	
B (dB/cm)	0.1894	0.0547	0.2575	
corr. coef.	0.9967	0.8419	0.7681	
clear conditions				
(calculated from 937 a priori radiosondes)				
A (dB)	0.0373	0.0821	0.1355	
B (dB)	0.1811	0.0643	0.3244	
corr. coef.	0.9717	0.8205	0.9732	
cloudy conditions				
(L > 0.0033 cm)				
(N = 2166)				
C (dB)	-0.0030	-0.0065	0.0136	
D (dB/cm)	4.5601	10.3796	38.9128	
corr. coef.	0.9999	0.9999	0.9728	
cloudy conditions				
(calculated from 500 a priori radiosondes; cloud liquid determined from a cloud model)				
C (dB)	0.0028	0.0074	-0.0812	
D (dB/cm)	4.5166	10.1190	52.9839	
corr. coef.	0.9922	0.9951	0.9954	

Table 5. Regression relations between absorption (dB) at 20.6, 31.65, and 90.0 GHz. San Nicolas Island, California, July 1987. Values in parentheses following the equations are standard error of estimate, the correlation coefficient, and 100 x standard error of estimate/mean, respectively.

---

clear conditions

(N = 3417)

$$\begin{aligned}\tau(20.6) &= -0.271 - 0.055 \tau(90.0) + 0.266 \tau(31.65), (0.011, 0.986, 3.5) \\ \tau(31.65) &= 0.086 + 0.141 \tau(90.0) + 0.162 \tau(20.6), (.003, 0.995, 1.1) \\ \tau(90.0) &= -0.332 - 0.107 \tau(20.6) + 4.50 \tau(31.65), (0.015, 0.991, 2.2)\end{aligned}$$

cloudy conditions

(L > 0.0025 cm)

(N = 14162)

$$\begin{aligned}\tau(20.6) &= -0.044 - 0.890 \tau(90.0) + 5.72 \tau(31.65), (0.041, 0.933, 6.3) \\ \tau(31.65) &= 0.093 + 0.172 \tau(90.0) + 0.089 \tau(20.6), (0.005, 0.999, 1.4) \\ \tau(90.0) &= -0.539 - 0.460 \tau(20.6) + 5.73 \tau(31.65), (0.029, 0.998, 2.1)\end{aligned}$$

all data

(N = 24129)

$$\begin{aligned}\tau(20.6) &= -0.385 - 0.849 \tau(90.0) + 5.43 \tau(31.65), (0.039, 0.939, 9.7) \\ \tau(31.65) &= 0.087 + 0.175 \tau(90.0) + 0.092 \tau(20.6), (0.005, 0.999, 1.6) \\ \tau(90.0) &= -0.499 - 0.463 \tau(20.6) + 5.64 \tau(31.65), (0.029, 0.998, 2.5)\end{aligned}$$

Table 6. Regression relations between absorption (dB) at 20.6, 31.65, and 90.0 GHz. Denver, Colorado, December, 1987. The numbers in parentheses following the equations are the standard error of estimate, the correlation coefficient, and 100 x standard error of estimate/mean, respectively.

---

clear conditions

(N = 12105)

$$\begin{aligned}\tau(20.6) &= -0.272 - 0.203 \tau(90.0) + 3.57 \tau(31.65), (0.024, 0.889, 16.1) \\ \tau(31.65) &= 0.076 + 0.136 \tau(90.0) + 0.108 \tau(20.6), (0.004, 0.972, 3.0) \\ \tau(90.0) &= -0.396 - 0.252 \tau(20.6) + 5.57 \tau(31.65), (0.026, 0.958, 8.2)\end{aligned}$$

cloudy conditions

(L > 0.0033 cm)

(N = 2166)

$$\begin{aligned}\tau(20.6) &= 0.055 + 0.047 \tau(90.0) + 0.443 \tau(31.65), (0.028, 0.956, 12.6) \\ \tau(31.65) &= 0.019 + 0.178 \tau(90.0) + 0.455 \tau(20.6), (0.028, 0.981, 10.0) \\ \tau(90.0) &= -0.207 + 0.892 \tau(20.6) + 3.27 \tau(31.65), (0.122, 0.958, 13.3)\end{aligned}$$

all data

(N = 14181)

$$\begin{aligned}\tau(20.6) &= 0.084 + 0.139 \tau(90.0) + 0.107 \tau(31.65), (0.040, 0.802, 25.2) \\ \tau(31.65) &= 0.056 + 0.242 \tau(90.0) + 0.014 \tau(20.6), (0.014, 0.984, 9.0) \\ \tau(90.0) &= -0.229 + 0.279 \tau(20.6) + 3.78 \tau(31.65), (0.056, 0.985, 13.7)\end{aligned}$$

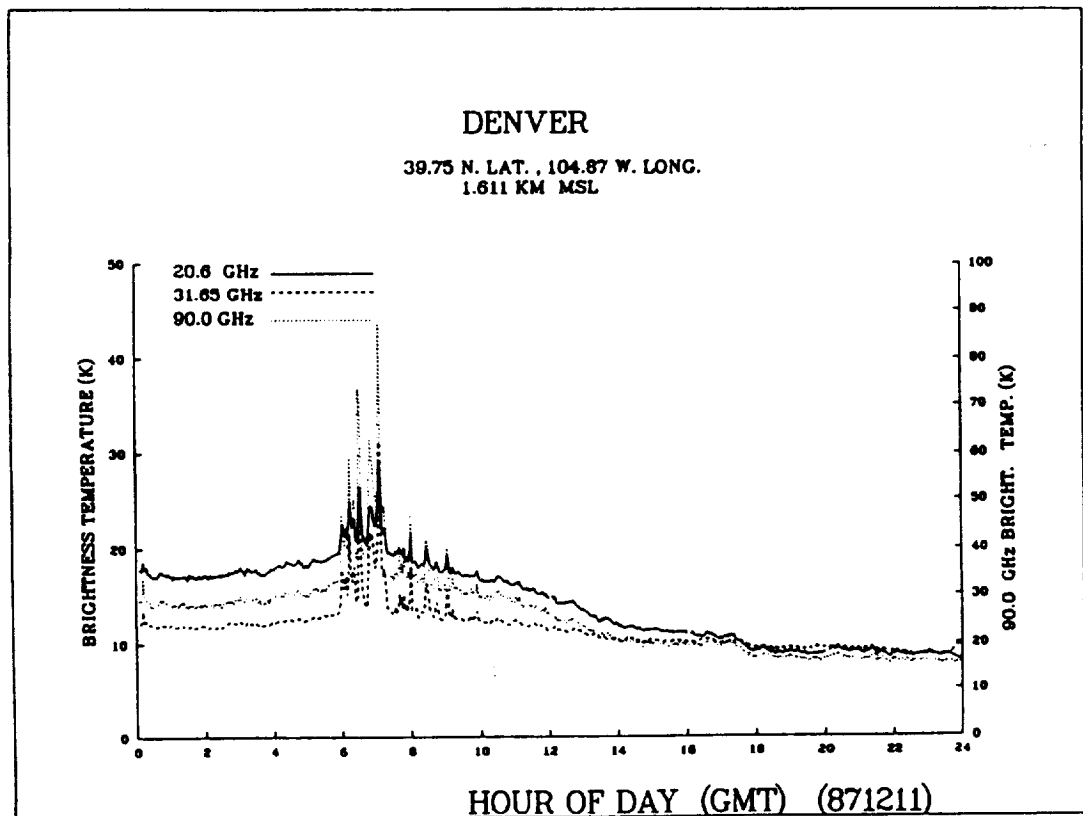
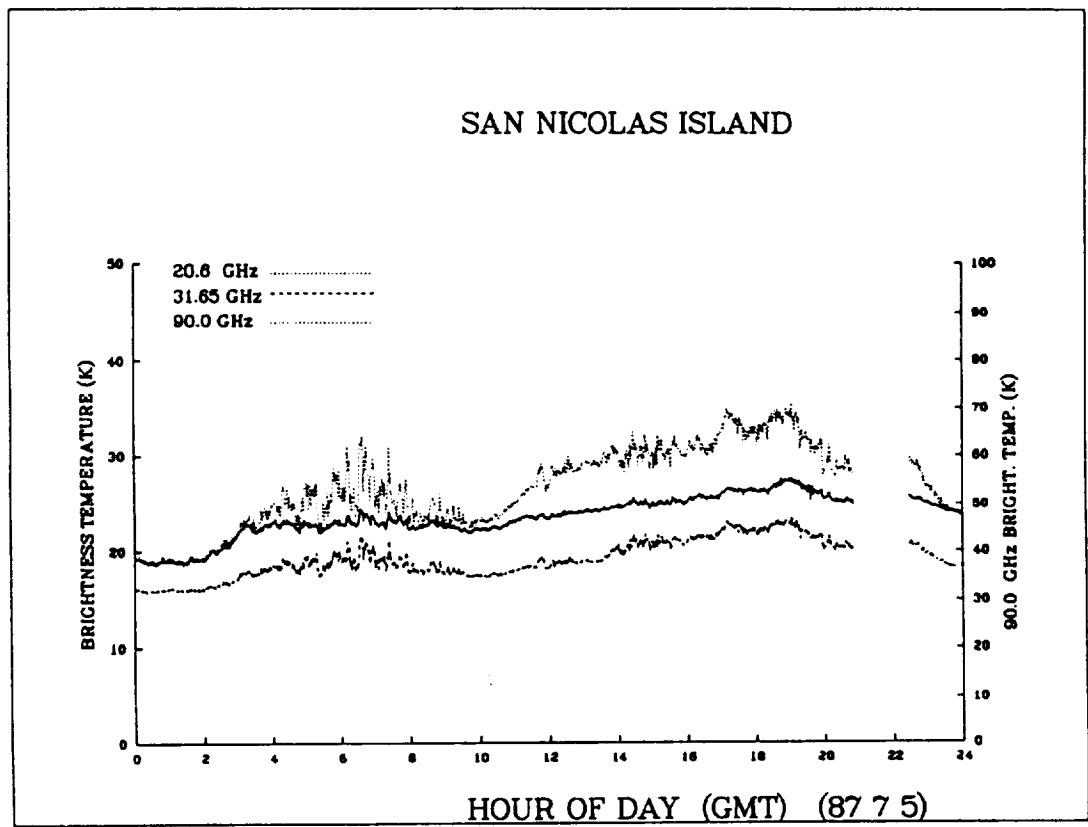


Fig. 1. Time series of brightness temperatures measured by 3 channel radiometer at San Nicolas Island and Denver.

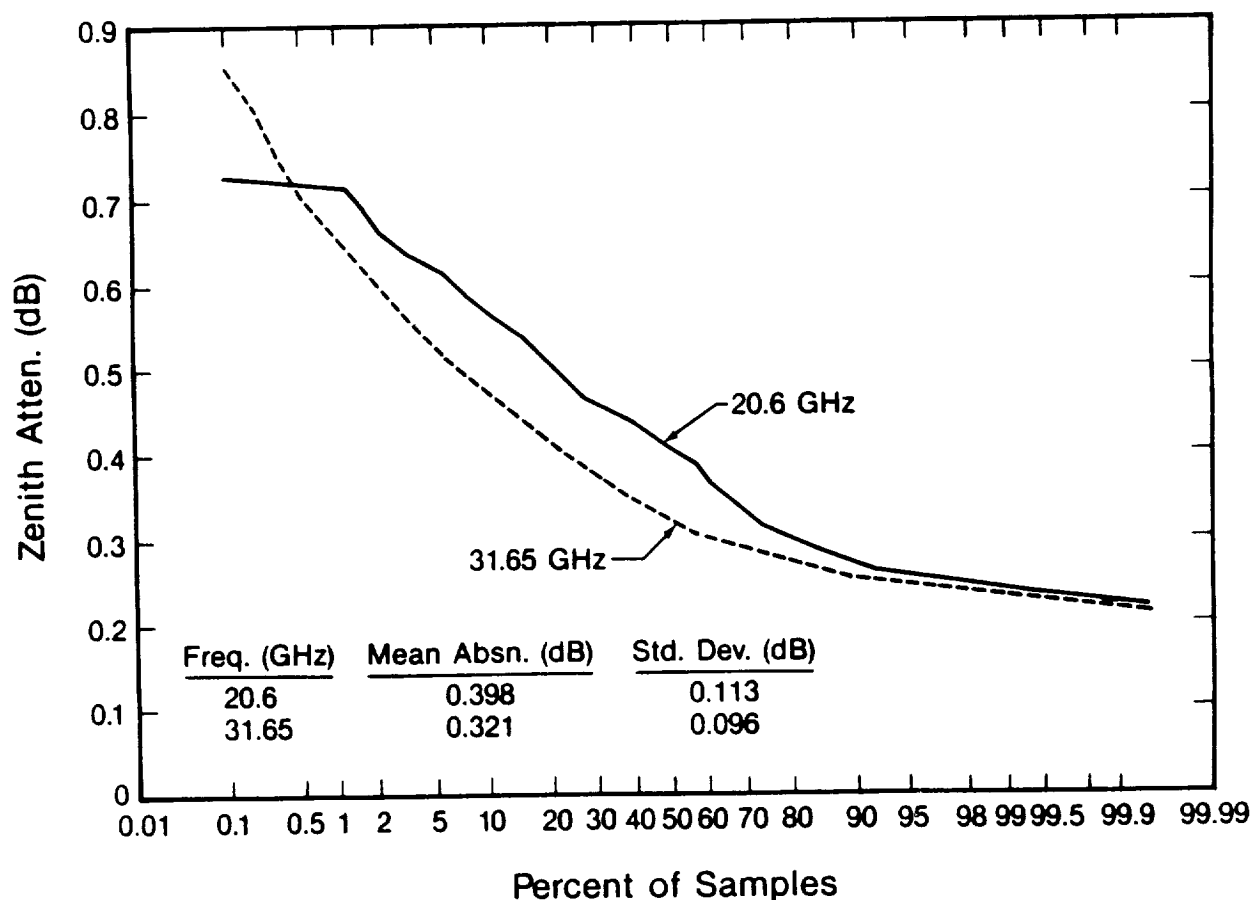
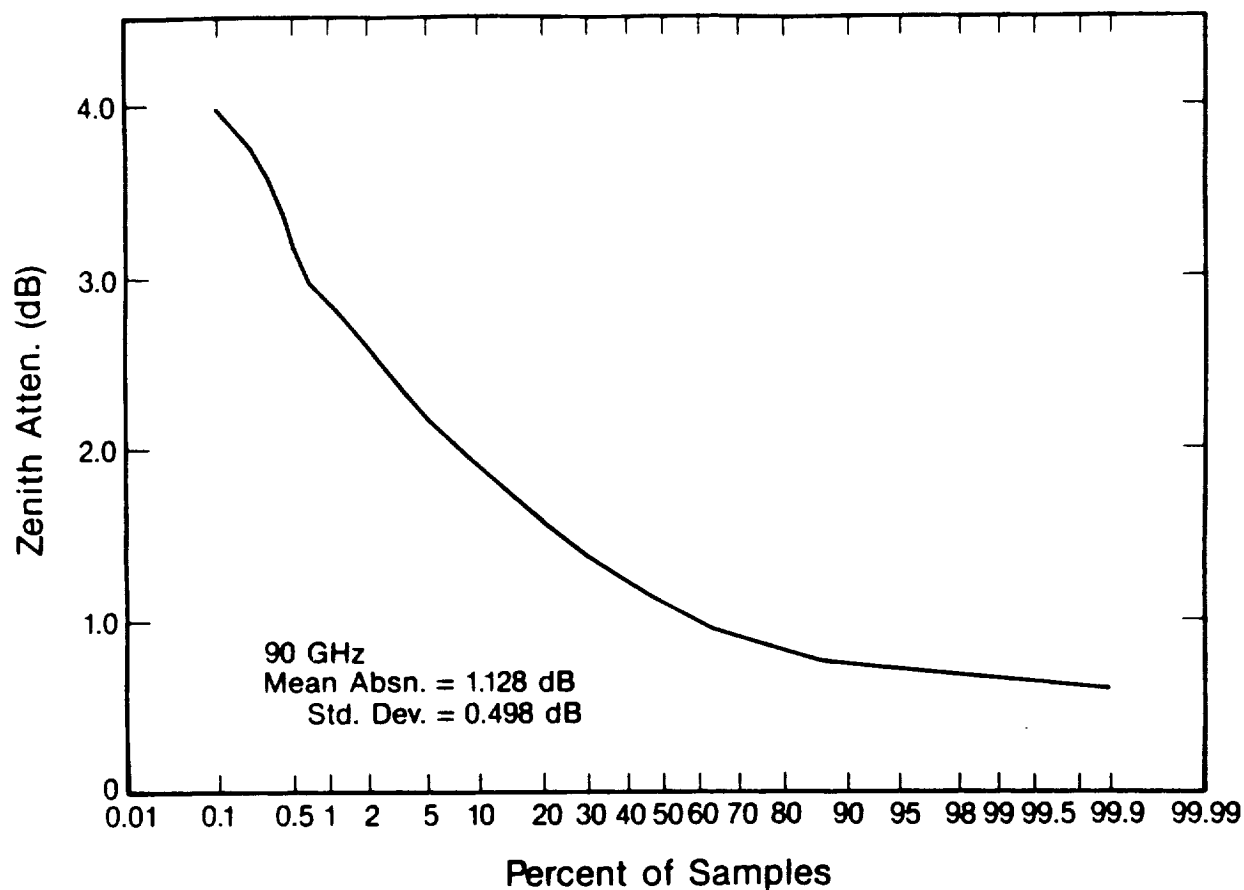


Fig. 2. Cumulative distribution of zenith attenuation measured by 3 channel radiometer at San Nicolas Island, July 1987. 4805 five-minute averages.

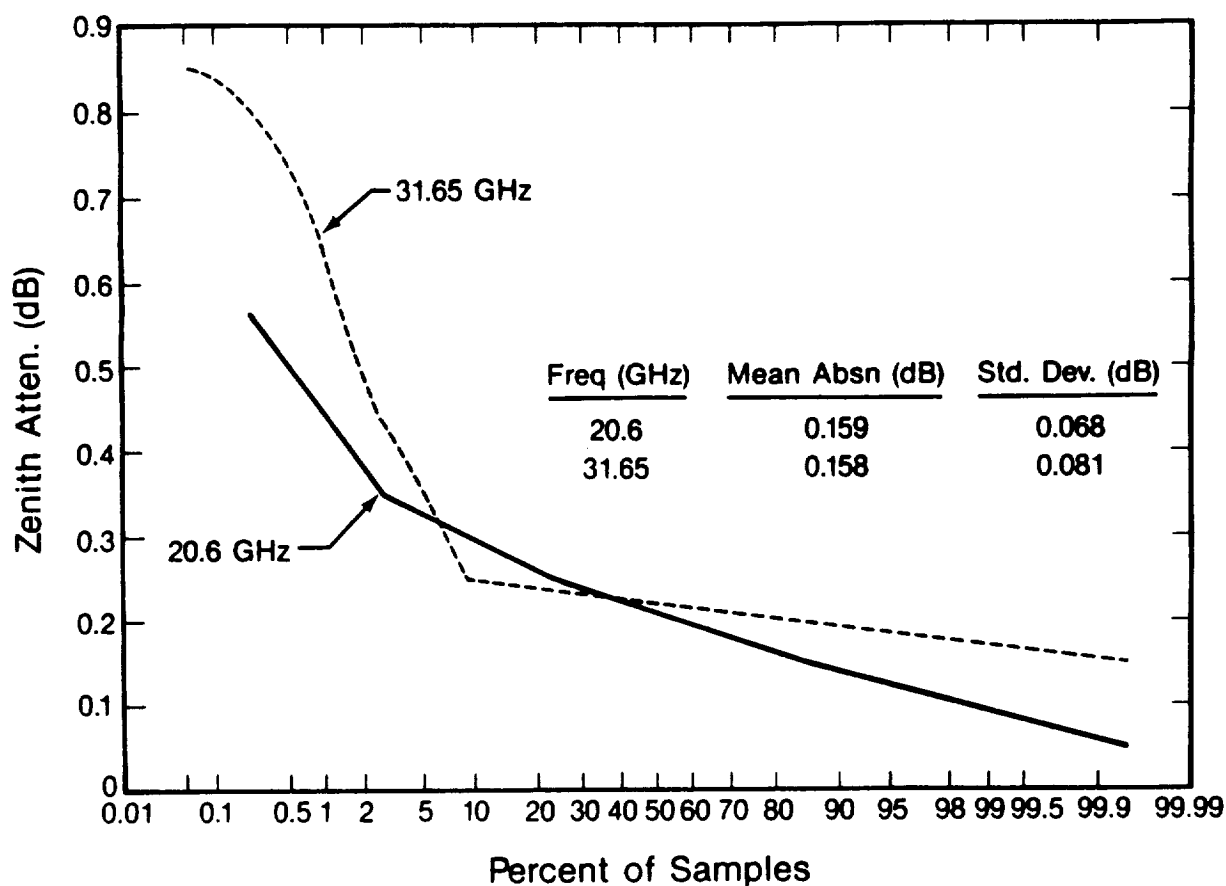
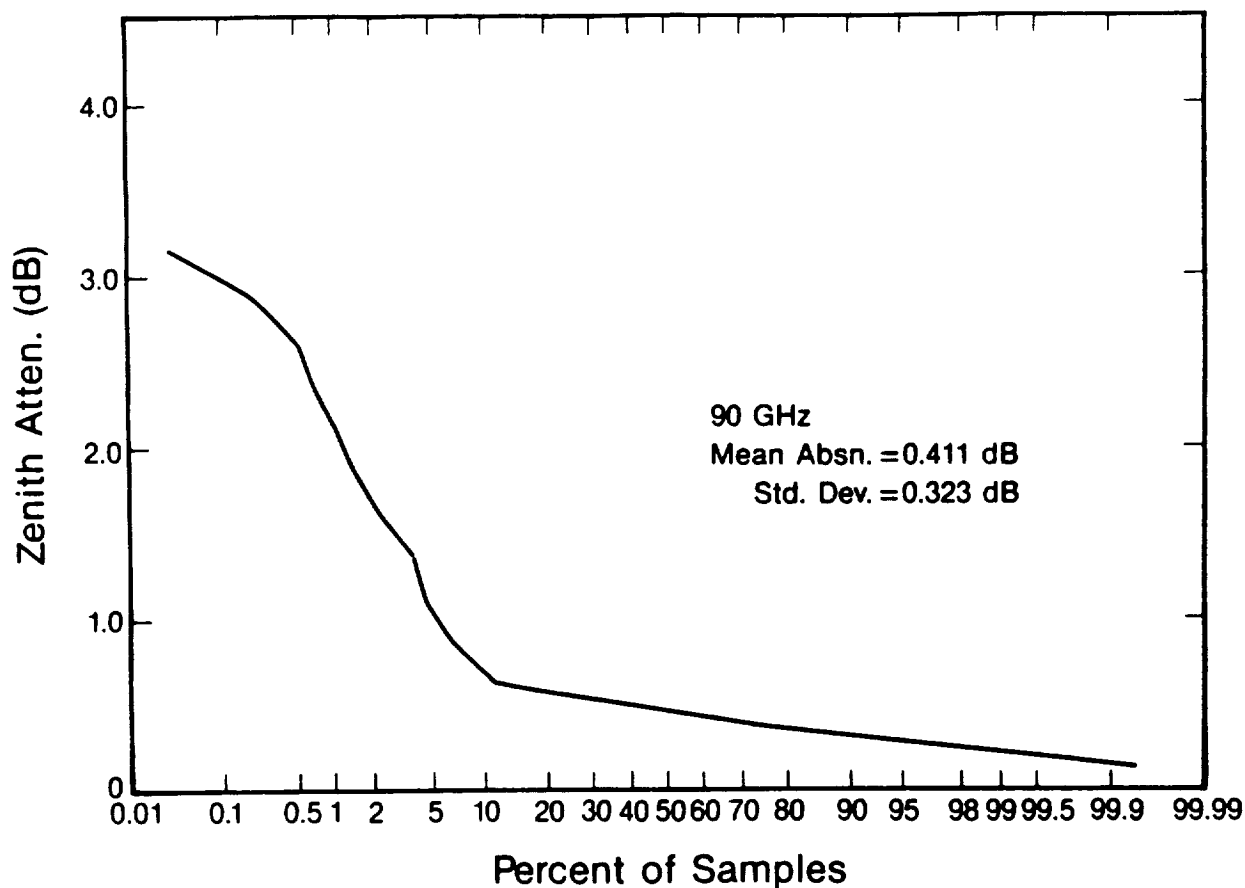


Fig. 3. Cumulative distribution of zenith attenuation measured by 3 channel radiometer at Denver, Colorado, December 1987. 14181 two-minute averages.